Heptanuclear Heterometallic [Cu$_6$Ln] Clusters: Trapping Lanthanides into Copper Cages with Artificial Amino Acids

George J. Sopasis,[†,§] Angelos B. Canaj,[†] Aggelos Philippidis,[⊥] Milosz Siczek,[‡] Tadeusz Lis,[‡] James R. O'Brien,[‖] Manolis M. Antonakis,[†] Spiros A. Pergantis,[†] and Constantinos J. Milios*[,†]

[†]Department of Chemistry, The University of Crete, Voutes, 71003, Herakleion, Greece

[§]Department of Materials Science and Technology, The University of Crete, Voutes, 71003, Herakleion, Greece

[⊥]Institute of Electronic Structure and Laser, Foundation for Research and Technology-Hellas (IESL-FORTH), P.O. Box 1385, GR 711 10 Herakleion, Crete, Greece

[‡]Faculty of Chemistry, University of Wroclaw, Joliot-Curie 14, 50-383 Wroclaw, Poland

[‖]Quantum Design, San Diego, California 92121, United States

S *Supporting Information*

ABSTRACT: Employment of the artificial amino acid 2-amino-isobutyric acid, aibH, in Cu^{II} and Cu^{II}/Ln^{III} chemistry led to the isolation and characterization of 12 new heterometallic heptanuclear [Cu$_6$Ln(aib)$_6$(OH)$_3$(OAc)$_3$(NO$_3$)$_3$] complexes consisting of trivalent lanthanide centers within a hexanuclear copper trigonal prism (aibH = 2-amino-butyric acid; Ln = Ce (**1**), Pr (**2**), Nd (**3**), Sm (**4**), Eu (**5**), Gd (**6**), Tb (**7**), Dy (**8**), Ho (**9**), Er (**10**), Tm (**11**), and Yb (**12**)). Direct current magnetic susceptibility studies have been carried out in the 5−300 K range for all complexes, revealing the different nature of the magnetic interactions between the 3d−4f metallic pairs: dominant antiferromagnetic interactions for the majority of the pairs and dominant ferromagnetic interactions for when the lanthanide center is Gd^{III} and Dy^{III}. Furthermore, alternating current magnetic susceptibility studies reveal the possibility of single-molecule magnetism behavior for complexes **7** and **8**. Finally, complexes **2**, **5−8**, **10**, and **12** were analyzed using positive ion electrospray mass spectrometry (ES-MS), establishing the structural integrity of the heterometallic heptanuclear cage structure in acetonitrile.
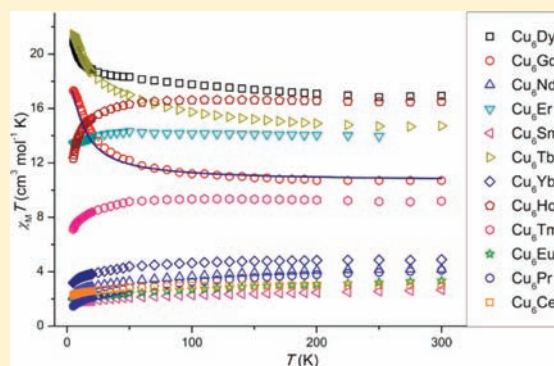
■ INTRODUCTION

Understanding the way metals magnetically "communicate" with each other when present in a metallic complex is of great importance, since over the last years numerous metallic complexes have found potential applications in many fields of science and technology.[1] For instance, in the field of molecular magnetism, and in particular in single-molecule magnetism (SMM), new compounds have been synthesized that can now retain their magnetization above or at liquid He temperatures,[2] while both homo- and heterometallic clusters have been reported to function as molecular refrigerants.[3] Therefore it becomes evident that for scientists to be able to understand and, consequently, control the nature of the magnetic interactions, *J*, between various metal centers is crucial, since the spin of the ground state of the complex, *S*, is dictated by such intermetallic interactions. Yet, this task is not trivial because for the vast majority of the metallic clusters, and especially those of high nuclearity, the quantitative analysis of the magnetic data is hindered by computational restrictions or overparameterization factors.

Although the investigation of the magnetic exchange interactions between 3d and 4f metal atoms started many years ago,[4] it now seems to be more topical than ever.[5] The reason lanthanides are now considered as major candidates in the molecular magnetism field is due to (i) their large magnetic moments and (ii) their spin−orbit coupling based magnetic anisotropy (with the exceptions of La^{III}, Gd^{III}, and Lu^{III}). Their main disadvantage though seems to be the promotion of weak exchange interactions due to the shielding of the 4f electrons by the outer 5s and 5p electrons.

Furthermore, lanthanide-based clusters find applications as light-emitting diodes, optical fibres, lasers, optical amplifiers, NIR-emitting materials, and sensory probes.[6] This is because the electronic properties of the lanthanide ions are well retained upon complex formation, due to the shielding of the inner 4f electrons by the outer 5s and 5p electrons, leading to a very weak ligand field effect.

Following our initial work with the employment of artificial amino acid ligands for the construction of heterometallic Ni^{II}−Ln[7] and Co^{II}−Ln[8] clusters, we herein extend our efforts toward the synthesis and characterization of heterometallic Cu^{II}−Ln complexes. Therefore, we report the synthesis and magnetic

properties of 12 new $[Cu^{II}_6Ln^{III}]$ clusters based on the use of 2-aminoisobutyric acid, aibH (Scheme 1).

Scheme 1. Structural Formulae of aibH (Left) and Its Coordination Mode in 1−12

aibH
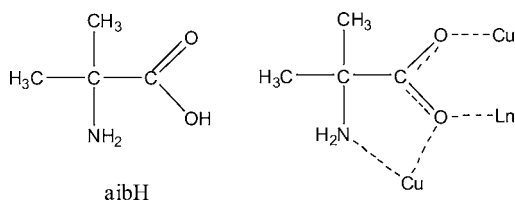
■ EXPERIMENTAL SECTION

All manipulations were performed under aerobic conditions, using materials as received (reagent grade). *CAUTION! Although no problems were encountered in this work, care should be taken when using the potentially explosive perchlorate anions.* Elemental analyses (C, H, N) were performed by the University of Ioannina microanalysis service. Variable-temperature, solid-state direct current (dc) magnetic susceptibility data down to 1.8 K were collected on a Quantum Design MPMS-XL SQUID magnetometer (University of Crete) equipped with a 5 T dc magnet for complexes. Diamagnetic corrections were applied to the observed paramagnetic susceptibilities using Pascal's constants.

Electrospray mass spectrometry was conducted using an ion trap mass spectrometer (Thermo Scientific LCQ Advantage). Samples were infused directly into the source at 3 μL min^{-1} using the built-in syringe pump. Data were typically collected in the full scan mode, with a range of m/z from 200 to 2000, in the positive ionization mode. The sheath and auxiliary gas was nitrogen. All ES-MS measurements were performed in acetonitrile solutions.

General Synthetic Procedure for Complexes 1−12. All complexes were prepared from the reaction of $Cu_2(OAc)_4\cdot2H_2O$ with aibH and the corresponding $Ln(NO_3)_3\cdot6H_2O$ in the presence of NMe$_4$OH in MeOH. The crystals were obtained by layering with Et$_2$O after 2 days in good yields (∼50%). All crystals were dried *in vacuo* and analyzed as solvent-free. Elemental Anal. Calcd (Found) for **1**, C 23.27 (23.18), H 3.91 (3.73), N 8.14 (8.27); **2**, C 23.26 (23.37), H 3.90 (3.73), N 8.14 (8.07); **3**, C 23.21 (23.09), H 3.90 (3.65), N 8.12 (8.21); **4**, C 23.12 (23.21), H 3.88 (3.69), N 8.09 (8.03); **5**, C 23.10 (23.01), H 3.88 (3.72), N 8.08 (8.17); **6**, C 23.02 (22.93), H 3.86 (3.61), N 8.05 (8.17); **7**, C 22.99 (22.86), H 3.86 (3.71), N 8.04 (8.13); **8**, C 22.94 (22.87), H 3.85 (3.59), N 8.03 (8.15); **9**, C 22.91 (23.03), H 3.84 (3.61), N 8.01 (7.89); **10**, C 22.87 (22.97), H 3.84 (3.65), N 8.00 (7.88); **11**, C 22.85 (22.73), H 3.83 (3.57), N 7.99 (8.11); **12**, C 22.79 (22.88), H 3.82 (3.69), N 7.97 (7.84).

X-ray Crystallography. Diffraction data for complexes **1−12** were collected on an Xcalibur PX or KM4 diffractometer. The structures were solved by direct methods and refined by full-matrix least-squares techniques on F^2 with SHELXL.[9] Data collection parameters and structure solution and refinement details are listed in Tables 1−3. Full details can be found in the CIF files provided in the Supporting Information.

■ RESULTS AND DISCUSSION

Synthesis. All 12 complexes contain six Cu^{II} and one Ln^{III} ions. The $[Cu_6Ln]$ metallic core forms upon the reaction of $Cu_2(OAc)_4\cdot2H_2O$ with $Ln(NO_3)_3\cdot6H_2O$ and 1 equiv of aibH in MeOH in the presence of base, according to eq 1:

$$3Cu_2(OAc)_4\cdot2H_2O + Ln(NO_3)_3\cdot6H_2O + 6aibH$$
$$+ 3OH^- \xrightarrow{MeOH} [Cu_6Ln(aib)_6(OH)_3(OAc)_3(NO_3)_3]$$
$$+ 6OAcH + 3OAc^- + 12H_2O \qquad (1)$$
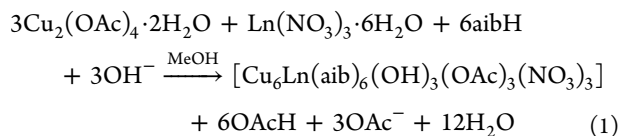
Table 1. Crystallographic Data for Complexes 1−5

	1·3CH$_3$OH·1.5Et$_2$O·0.3H$_2$O	2·5.25CH$_3$OH·1.5Et$_2$O·0.1H$_2$O	3·6.75CH$_3$OH·1.5Et$_2$O·0.1H$_2$O	4·1.5Et$_2$O·6.75CH$_3$OH·0.1H$_2$O	5·6.75CH$_3$OH·1.5Et$_2$O
formula[a]	C$_{39}$H$_{87.6}$CeCu$_6$N$_9$O$_{34.8}$	C$_{41.25}$H$_{96.2}$Cu$_6$N$_9$O$_{36.85}$Pr	C$_{42.75}$H$_{102.2}$Cu$_6$N$_9$NdO$_{38.35}$	C$_{42.75}$H$_{102.2}$Cu$_6$N$_9$O$_{38.35}$Sm	C$_{42.75}$H$_{102}$Cu$_6$EuN$_9$O$_{38.25}$
M_W	1760.94	1830.22	1881.61	1887.72	1887.53
cryst syst	hexagonal	hexagonal	hexagonal	hexagonal	hexagonal
space group	$P6_3/m$	$P6_3/m$	$P6_3/m$	$P6_3/m$	$P6_3/m$
a, Å	20.130(5)	19.892(7)	19.880(8)	19.858(6)	19.827(4)
c, Å	13.367(4)	13.304(5)	13.243(5)	13.230(4)	13.258(3)
V, Å^3	4691(2)	4559(3)	4533(3)	4518(2)	4513.6(16)
Z	2	2	2	2	2
T, K	100	100	100	100	100
λ, Å	0.71073	0.71073	0.71073	0.71073	0.71073
D_c, g cm^{-3}	1.247	1.333	1.379	1.388	1.389
μ(Mo Kα), mm^{-1}	1.88	1.97	2.02	2.10	2.15
meas/indep (R_{int}) reflns	41589/7660 (0.037)	27265/3993 (0.063)	18036/4142 (0.044)	30838/4587 (0.075)	28619/4582 (0.045)
obsd reflns [$I > 2\sigma(I)$]	5964	2805	3016	3298	3467
$wR2^b$	0.164	0.134	0.179	0.148	0.141
R1^c	0.050	0.048	0.072	0.065	0.054
GOF on F^2	1.113	1.072	1.144	1.094	1.100
$\Delta\rho_{max,min}$, e Å^{-3}	1.79, −1.27	1.11, −0.70	1.75, −1.85	1.46, −1.42	2.68, −1.04

[a]Including solvate molecules. [b]$wR2 = [\sum w(|F_o^2| - |F_c^2|)^2/\sum w|F_o^2|^2]^{1/2}$. [c]$R1 = \sum ||F_o| - |F_c||/\sum |F_o|$. For observed data.

Table 2. Crystallographic Data for Complexes 6–10

	6·1.5Et$_2$O·4.5CH$_3$OH·1.125H$_2$O	7·1.5CH$_3$OH·1.5H$_2$O	8·3CH$_3$OH·1.5Et$_2$O	9·6.75CH$_3$OH·1.5Et$_2$O	10·1.5Et$_2$O·6.75CH$_3$OH·0.1H$_2$O
formula[a]	C$_{40.5}$H$_{95.25}$Cu$_6$GdN$_9$O$_{37.125}$	C$_{31.50}$H$_{69}$Cu$_6$N$_9$O$_{33}$Tb	C$_{39}$H$_{87}$Cu$_6$DyN$_9$O$_{34.50}$	C$_{42.75}$H$_{102}$Cu$_6$HoN$_9$O$_{38.25}$	C$_{42.75}$H$_{102.2}$Cu$_6$ErN$_9$O$_{38.35}$
M_W	1841.00	1642.12	1777.92	1900.50	1904.64
cryst syst	hexagonal	hexagonal	hexagonal	hexagonal	hexagonal
space group	$P6_3/m$	$P6_3/m$	$P6_3/m$	$P6_3/m$	$P6_3/m$
a, Å	19.929(6)	20.013(9)	20.116(5)	19.802(6)	19.955(4)
c, Å	13.308(4)	13.260(3)	13.338(5)	13.224(4)	13.273(3)
V, Å^3	4577(2)	4599(3)	4674(2)	4491(2)	4577.2(17)
Z	2	2	2	2	2
T, K	100	200	120	100	100
λ, Å	0.71073	0.71073	0.71073	0.71073	0.71073
D_c, g cm^{-3}	1.336	1.186	1.263	1.406	1.382
μ(Mo Kα), mm^{-1}	2.15	2.18	2.19	2.34	2.35
meas/indep (R_{int}) reflns	16916/4625 (0.032)	18505/4691 (0.079)	49635/5421 (0.058)	16148/3629 (0.030)	65078/7005 (0.066)
obsd reflns [$I > 2\sigma(I)$]	3603	2507	4186	3078	5003
$wR2$[b]	0.109	0.245	0.144	0.113	0.148
$R1$[d]	0.033	0.098	0.047	0.045	0.060
GOF on F^2	1.004	1.064	1.11	1.123	1.114
$\Delta\rho_{max,min}$, e Å^{-3}	0.99, −0.53	2.22, −2.08	2.18, −0.93	1.21, −0.86	3.19, −1.72

[a]Including solvate molecules. [b]$wR2 = [\sum w(|F_o{}^2| - |F_c{}^2|)^2/\sum w|F_o{}^2|^2]^{1/2}$. For observed data. [d]$R1 = \sum||F_o| - |F_c||/\sum|F_o|$.

Table 3. Crystallographic Data for Complexes 11 and 12

	11·6.75CH$_3$OH·1.5Et$_2$O	12·3CH$_3$OH·1.5Et$_2$O·0.1H$_2$O
formula[a]	C$_{42.75}$H$_{102}$Cu$_6$N$_9$O$_{38.25}$Tm	C$_{39}$H$_{87.2}$Cu$_6$N$_9$O$_{34.6}$Yb
M_W	1904.50	1790.26
cryst syst	hexagonal	hexagonal
space group	$P6_3/m$	$P6_3/m$
a, Å	19.852(7)	19.965(5)
c, Å	13.239(4)	13.193(4)
V, Å^3	4518(3)	4554(2)
Z	2	2
T, K	100	100
λ, Å	0.71073	0.71073
D_c, g cm^{-3}	1.400	1.306
μ(Mo Kα), mm^{-1}	2.43	2.46
meas/indep (R_{int}) reflns	41729/4589 (0.067)	29909/4241 (0.053)
obsd reflns [$I > 2\sigma(I)$]	3448	3300
$wR2$[b]	0.133	0.164
$R1$[d]	0.055	0.064
GOF on F^2	1.140	1.235
$\Delta\rho_{max,min}$, e Å^{-3}	2.29, −1.35	1.26, −1.89

[a]Including solvate molecules. [b]$wR2 = [\sum w(|F_o{}^2| - |F_c{}^2|)^2/\sum w|F_o{}^2|^2]^{1/2}$. For observed data. [d]$R1 = \sum||F_o| - |F_c||/\sum|F_o|$.

The formation of the complexes can be considered as the break down of a "Ln(NO)$_3$" unit and the encapsulation of its ingredients into a [Cu$_6$] cage formed by the use of the aib$^-$ linkers. The presence of the base is crucial for the formation of the products, since besides deprotonating the aibH ligands it provides the three hydroxide groups found in the complexes; when no base was used the only crystalline material we managed to isolate was unreacted "Cu$_2$(OAc)$_4$·2H$_2$O" as evidenced by IR spectroscopy. In order to examine whether the nature of the base or the solvent affects the identity of the product, we repeated the reactions using various bases, such as NEt$_3$, NMe$_4$OH, and NaOH, and various alcoholic solvents, but all reactions formed crystalline products displaying the

same XRD powder spectrum with the single-crystals solved. Furthermore, we checked whether the time duration of the reaction could lead to different products, but again all our attempts were not fruitfull since all products isolated displayed the same IR spectrum with the corresponding [Cu$_6$Ln] complexes. This strongly suggests that the clusters seem to be the thermodynamically favored end-products of these reactions under a wide spectrum of reaction conditions.

In order to further support the analysis of the complexes we performed energy dispersive X-ray spectroscopy analysis (EDS) in bulk crystalline material of complex 7 in order to verify the ratio of Cu/Tb. The ratio was found 5.83:1, that is, very close to the one established by single-crystal X-ray crystallography of 6:1 (Figure 1).
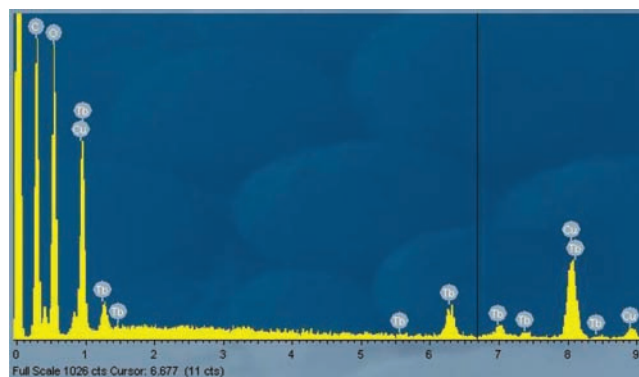

Figure 1. EDS analysis of complex 7.

A detailed CCDC search revealed 15 heterometallic heptanuclear [Cu$_6$Ln] complexes that have been isolated and reported in the past.[10] Furthermore, this is only the second example in which the aibH ligand is used for the construction of Cu/Ln complexes, since an impressive [Cu$_{24}$Gd$_6$] complex, [Cu$_{24}$Gd$_6$(OH)$_{30}$(aib)$_{16}$(ClO$_4$)(H$_2$O)$_{22}$](ClO$_4$)$_{17}$(OH)$_2$(H$_2$O)$_{20}$, has been previously reported.[11] It is really interesting that the triacontanuclear heterometallic cluster was constructed by the use of Cu(ClO$_4$)$_2$·6H$_2$O vs Cu$_2$(OAc)$_4$·2H$_2$O in our case.

It seems that the three OAc⁻ present in our structures function as "capping" ligands inhibiting the further growth of the [Cu₆Ln] metallic core.

Description of Structures. Selected interatomic distances and angles are listed in Tables S1−S12, Supporting Information for complexes **1**−**12**. All complexes **1**−**12** are essentially isostructural, and so for the sake of brevity, we provide only the description of the $[Cu_6Gd(aib)_6(OH)_3(OAc)_3(NO_3)_3]$ cluster, **6** (Figure 2). Its metallic core consists of six Cu^{II} ions
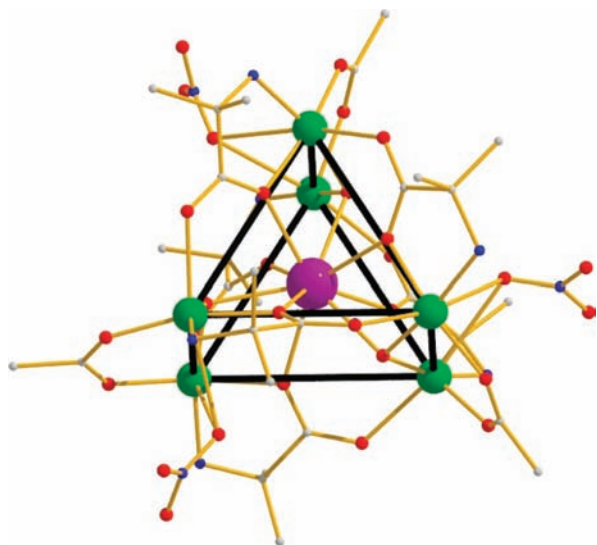
Figure 2. The "generic" molecular structure of complexes **1**−**12**. Color code: Cu^{II} = green; Gd^{III} = deep purple; O = red; N = blue; C = white.

arranged at the corners of a trigonal prism, which encapsulates one Ln^{III} via six $\eta^2{:}\eta^1{:}\eta^1{:}\mu_3$ deprotonated aib⁻ ligands with each one bridging two Cu^{II} ions and the Ln^{III} center, and three μ_3-OH⁻ ligands each one bridging two Cu^{II} ions and the Ln^{III} center. Furthermore, there are three monatomic μ-NO₃⁻ groups responsible for bridging the three [Cu₂] pairs located at the corners of the trigonal prism. Finally, three bridging $\eta^1{:}\eta^1{:}\mu$ OAc⁻ groups fill the coordination spheres of the Cu^{II} ions. Surprisingly, no solvate molecules were found coordinated on the metal ions. Each Cu^{II} ion is six-coordinate adopting Jahn−Teller distorted octahedral geometry, as expected for a high-spin 3d^9 ion, with the O$_{NO_3^-}$ and the O$_{COO^-}$ of the $\eta^2{:}\eta^1{:}\eta^1{:}\mu_3$ aib⁻ ligands occupying the elongated JT positions on each Cu^{II}. The lanthanide ions are nine-coordinate, adopting a tricapped trigonal prismatic coordination environment. The base faces of the trigonal prism consist of two equilateral triangles with ∼5.3 Å edge, while the depth of the prism is ∼3.1 Å with the Cu^{II}⋯Ln^{III} distance in the 3.4 Å range.

In the crystal, there are no obvious interactions between the clusters. Each NO₃⁻ forms two H-bonds with its "free" O atoms and the N−H groups of two aib⁻ ligands, resulting in the formation of six H-bonds in the periphery of each cluster. Finally, the hydroxide groups form one H-bond with the noncoordinated MeOH solvate molecules (Figure 3).

Mass Spectroscopy. Positive ion (+) electrospray (ES) mass spectrometry (MS) was used to analyze complexes **2**, **5**−**8**, **10**, and **12** dissolved in an aprotic solvent, acetonitrile, in order to preserve complex integrity while allowing for electrospraying. Typically, in (+)-ES-MS, analyte molecular ions are observed as a result of the addition of a H⁺ to the analyte molecule. It is therefore common to provide excess
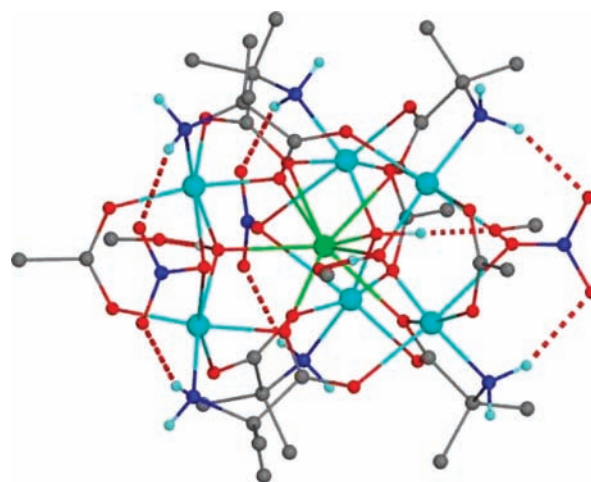

Figure 3. The H-bond pattern in **6**. Color code: Cu^{II} = cyan; Gd^{III} = green; O = red; N = blue; C = gray.

protons by adding small amounts of volatile acids to the sample solution. In the present study, the instability of the coordination complexes precluded the use of such an approach. However, even in the absence of charge carriers intense pseudomolecular ions, corresponding to the neutral complex minus a negatively charged nitrate ligand, [M − NO₃]⁺, were observed for all coordination complexes analyzed (Figure 4 shows the (+)-ES mass spectrum acquired for the Tb-containing complex **7**; typical ES mass spectra for the other six complexes analyzed can be found in Figure S1a−f, Supporting Information). In support of these assignments is the excellent match observed between the acquired distinct isotopic distributions for the [M − NO₃]⁺ ions and the theoretically calculated distributions (Figure 4, inset). It was also observed that in a few cases, for

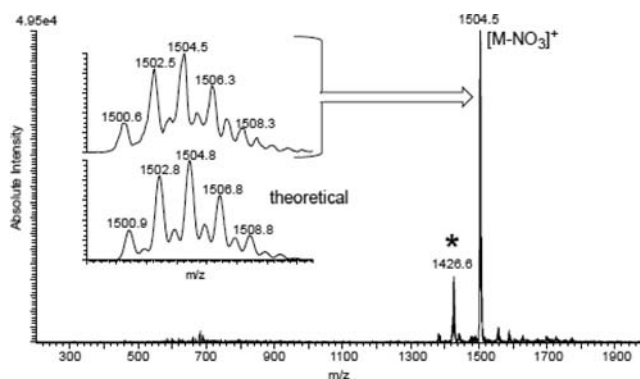**Figure 4.** (+)-ES mass spectrum of [Cu₆Tb] complex **7** in MeCN, acquired using a transfer capillary temperature of 176 °C and source-induced dissociation voltage of 5 V. Inset shows the zoomed region around the [M − NO₃]⁺ pseudomolecular ion (top) and theoretically calculated isotopic distribution (bottom). The asterisk indicates an observed fragment ion.

example, for complex **12** (Figure 5a), low intensity ion signals were observed for [M + Na]⁺ and [M + K]⁺ adduct ions, and even for [M + Cu]⁺. Because these metal ions were not added intentionally but were present possibly as a result of solvent and reagent impurities and reagent excess, the intensity of the formed adduct ions varied significantly from sample to sample. Because only a limited number of studies[12] have so far incorporated the successful use of ES-MS for the characterization of
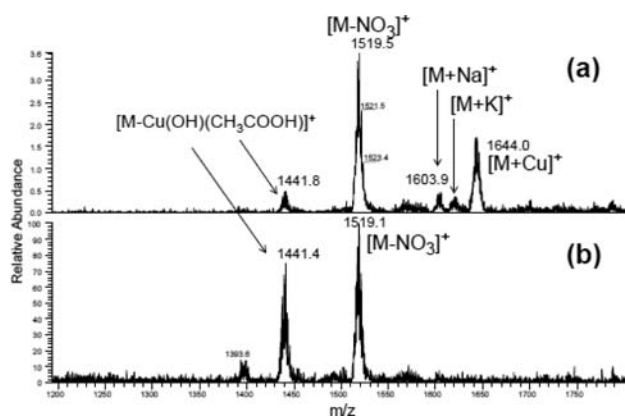
Figure 5. (+)-ES mass spectrum of Cu_6Yb complex **12** in MeCN; acquired with transfer capillary temperature of 150 °C (a) and 320 °C (b). Source-induced dissociation voltage at 10 V.
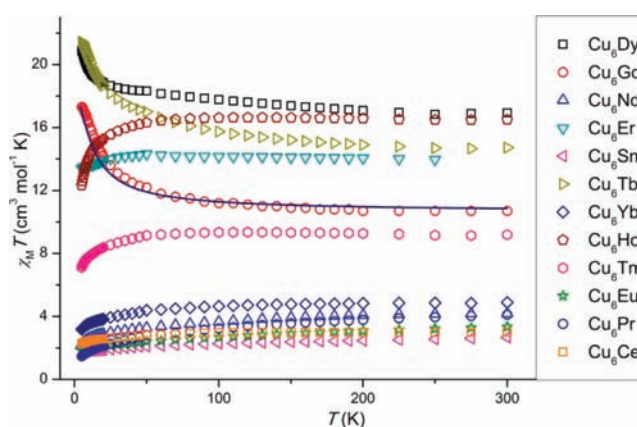

Figure 6. Plot of $\chi_M T$ vs T for complexes **1−12** under an applied dc field of 1000 G. The solid line represents a simulation of the data in the temperature range 5−300 K for complex **6** (see text).

Table 4. Theoretical and Experimentally Found $\chi_M T$ Values (cm³ mol⁻¹ K) for 1−12 (at 300 K)[a]

complex	g_j[13]	$\chi_M T_{theor}$	$\chi_M T_{exptl}$
[Cu_6Ce] (**1**)	0.86	3.62	2.99
[Cu_6Pr] (**2**)	0.80	4.42	4.11
[Cu_6Nd] (**3**)	0.73	4.51	4.18
[Cu_6Sm] (**4**)	0.28	2.91	2.66
[Cu_6Eu] (**5**)		2.82	3.44
[Cu_6Gd] (**6**)	2.00	10.70	10.69
[Cu_6Tb] (**7**)	1.50	14.62	14.61
[Cu_6Dy] (**8**)	1.33	16.94	16.74
[Cu_6Ho] (**9**)	1.25	16.86	15.50
[Cu_6Er] (**10**)	1.20	14.31	13.94
[Cu_6Tm] (**11**)	1.17	9.98	9.19
[Cu_6Yb] (**12**)	1.14	5.38	4.89

[a]Assuming a g-value of 2.24 for Cu^{II} and the corresponding g_j values for each Ln center.

large coordination compounds, we have investigated some of the ES parameters that seem to influence the behavior of the coordination complexes studied. To illustrate these findings, we have chosen to discuss the behavior of the Yb-containing complex **12**, even though similar behavior is observed for all complexes examined. Initially we studied the effect of the heated transfer capillary temperature on the coordination complex ions. In fact, in Figure 5, it is evident that a higher temperature causes severe compound fragmentation or thermal decomposition. More specifically the Cu cage seems to dissociate via the loss of a {Cu(OH)(CH₃COOH)} or {Cu(OH)(NO₃)} unit. At temperatures around or above 300 °C, the resulting fragment ion is of comparable intensity to the [M − NO₃]⁺ base peak. Overall, we observed that a suitable temperature range for maintaining molecular integrity, while obtaining high sensitivity, is between 150 and 200 °C. Also, identical fragmentation was observed when applying increased source accelerating voltage, >15 V (referred to as the source induced dissociation (sid) voltage on this particular instrument). Thus for the complexes studied here a sid of 0−10 V was determined to be optimum in order to avoid fragmentation.

Direct Current Magnetic Susceptibility Studies. Direct current magnetic susceptibility measurements were performed on polycrystalline samples of all complexes **1−12** in the 5−300 K range under an applied field of 0.1 T. The results are plotted as the $\chi_M T$ product vs T in Figure 6, while in Table 4, the theoretical and the experimentally found $\chi_M T$ values at room temperature for **1−12** are given for comparison. From a quick look, it becomes apparent that the 12 complexes can be divided in two categories: (i) those whose $\chi_M T$ value increases upon cooling, complexes **6**, **7**, and **8**, and (ii) those whose $\chi_M T$ value decreases upon cooling, complexes **1**, **2**, **3**, **4**, **5**, **9**, **10**, **11**, and **12**. Yet, this on its own is not conclusive regarding the magnetic interactions within the clusters, since for lanthanides the decrease of the $\chi_M T$ product upon cooling may be due to either antiferromagnetic interactions or depopulation of the Stark sublevels. From Table 4, we observe that the biggest percent deviation of the experimentally found $\chi_M T$ value from the theoretically expected one at room temperature is seen for complex **5**; this is because even though the Eu^{III} center in theory should not contribute to the magnetic moment of the complex, since its ground term is $^7F_0$ with $J = 0$, some contribution from thermally accessible levels such as $^7F_1$ and $^7F_2$ appears,[14] resulting in the large deviation between

the theoretical and experimental $\chi_M T$ values at room temperature.

We were able to successfully simulate the data for complex **6** adopting the 3-J model of Figure 7 and Hamiltonian eq 2 assuming the following: one (J_1) within the three pairs of Cu^{II}_2 centers (Cu1−Cu4, Cu2−Cu5 and Cu3−Cu6) mediated by an $\eta^1:\eta^1:\mu$ OAc⁻ ligand, a monatomic μ-NO₃⁻ bridge, and a μ_3-OH⁻ ligand, one (J_2) between the six peripheral Cu^{II} ions and the central Gd^{III} center, and, finally, one (J_3) within the six pairs of Cu^{II}_2 centers (Cu1−Cu2, Cu1−Cu3, Cu2−Cu3, Cu4−Cu5, Cu4−Cu6, and Cu5−Cu6) mediated by the carboxylate of the $\eta^2:\eta^1:\eta^1:\mu_3$ aib⁻ ligand in a *syn,anti*-fashion. Using the program MAGPACK and employing the Hamiltonian in eq 2

$$\hat{H} = -2J_1(\hat{S}_1 \cdot \hat{S}_4 + \hat{S}_2 \cdot \hat{S}_5 + \hat{S}_3 \cdot \hat{S}_6) - 2J_2(\hat{S}_1 \cdot \hat{S}_7 + \hat{S}_2 \cdot \hat{S}_7$$
$$+ \hat{S}_3 \cdot \hat{S}_7 + \hat{S}_4 \cdot \hat{S}_7 + \hat{S}_5 \cdot \hat{S}_7 + \hat{S}_6 \cdot \hat{S}_7)$$
$$- 2J_3(\hat{S}_1 \cdot \hat{S}_2 + \hat{S}_1 \cdot \hat{S}_3 + \hat{S}_2 \cdot \hat{S}_3 + \hat{S}_4 \cdot \hat{S}_5 + \hat{S}_4 \cdot \hat{S}_6 + \hat{S}_5 \cdot \hat{S}_6)$$
$$(2)$$

afforded the parameters $J_1 = -3.4$ cm⁻¹, $J_2 = 1.0$ cm⁻¹, $J_3 = 0.2$ cm⁻¹, and $g = 2.06$. The ground state of **6** was found to be $S = 13/2$ with the first and second excited state of $S = 11/2$ and $S = 9/2$, located only 0.4 cm⁻¹ and 0.7 cm⁻¹ above, respectively. The antiferromagnetic and rather small strength of J_1 may be
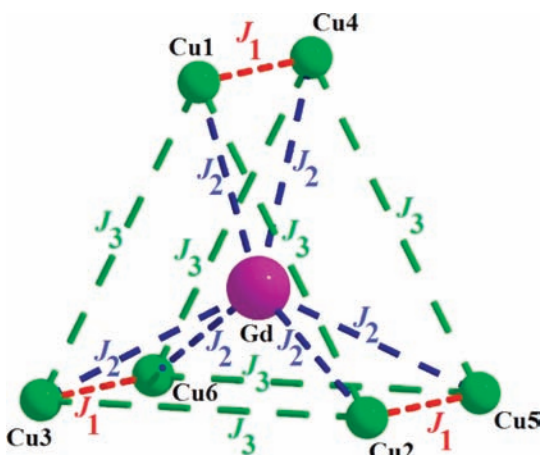
Figure 7. The *J*-interaction scheme employed for complex **6** (see text for details).

rationalized as following: the two Cu^{II} ions are located at ~3.12 Å distance, while the Cu−O(H)−Cu angle is ~109°. According to Hatfield and Hodgson, if the two Cu^{II} ions were only bridged by two OH^- ligands, then J_1 should be approximately −780 cm^{-1}.[15] But in our case, there is only one bridging OH^- and two additional bridging ligands: an η^1:η^1:μ OAc^- ligand and a monatomic μ-NO_3^- bridge, resulting in the lowering of the strength of J_1 as has been previously observed in $[Cu_2(OH)_2(dmaep)_2](ClO_4)_2$, in which the additional bridging of the Cu^{II} ions by two bidentate perchlorate anions lead to a *J* value of −4.8 cm^{-1} vs the theoretically expected value of approximately −50 cm^{-1},[16] probably due to the counter-complementarity effect between the bridging ligands, leading to a weak AF interaction.[17] Furthermore, to the best of our knowledge, this is the first example of a $[Cu^{II}_2]$ fragment bridged by a carboxylate, a hydroxide, and a nitrate ligand simultaneously. The ferromagnetic nature of J_2 is not surprising since it has been previously reported that the $Cu^{II}\cdots Gd^{III}$ interaction may well be ferromagnetic.[18] Finally, the weak ferromagnetic J_3 interaction is most probably due to the distance of the two Cu^{II} ions (~5.3 Å) and the *syn,anti* binding mode of the bridging carboxylate group of the η^2:η^1:η^1:μ_3 aib$^-$ ligand.[19]

Complex **8** hosts a central Dy^{III} ion, which has a $^6H_{15/2}$ ground state ($^6H_{15/2}$, $S = 5/2$, $L = 5$, $J = 15/2$, $g_j = 1.33$) with a first-order orbital momentum, which splits into eight Stark

components by the crystal field, each of them being a Kramers doublet. Upon cooling, the $\chi_M T$ value increases to reach the maximum value of 20.89 cm^3 mol^{-1} K at 5 K. In order to better understand the behavior of **8**, we synthesized and fully characterized the isostructural complex $[Zn_6Dy-(aib)_6(OH)_3(OAc)_3(NO_3)_3]$ (**13**, Figure SI2, Tables S13− S14, Supporting Information), and in Figure 8, we plot the $\chi_M T$ vs *T* for complexes **8** and **13** under an applied dc field of 1000 G, as well as the $\Delta\chi_M T$ vs *T* for these complexes. For **8**, the $\chi_M T$ value at 300 K is 16.74 cm^3 mol^{-1} K, and upon cooling, it stays constant until ~150 K, below which it increases slowly to a value of 18.67 cm^3 mol^{-1} K at ~25 K. Below 25 K, it increases rapidly to reach the maximum value of 20.89 cm^3 mol^{-1} K at 5 K. The magnetic behavior of **8** is governed by the intra-molecular magnetic exchange interactions, as well as the depopulation of the Dy^{III} Stark sublevels. On the other hand, for complex **13** the magnetic behavior is solely determined by the depopulation of the Stark sublevels; upon cooling, the Stark sublevels become progressively depopulated and at the lowest temperature only the ground Stark sublevel is populated. Therefore, the difference between the $\chi_M T_{[Cu_6Dy]} - \chi_M T_{[Zn_6Dy]}$ is a good qualitative indicator of the dominant intermolecular magnetic interactions within the $[Cu_6Dy]$ cluster. From Figure 8 (right) in the 125−300 K temperature range the $\Delta\chi_M T$ value is almost constant and equal to 2.82 cm^3 mol^{-1} K, which corresponds to the contribution of six isolated Cu^{II} ions, and below 125 K, it increases rapidly as the temperature is lowered, characteristic of dominant ferromagnetic interactions.[20]

Alternating Current Magnetic Susceptibility Studies. Alternating current magnetic susceptibility measurements were performed on polycrystalline samples of complexes **7** and **8** in the 1.8−10 K range in zero applied dc field and 1.0 G ac field oscillating in the 100−1000 Hz range. For both samples measured, the in-phase (χ_M', plotted as $\chi_M' T$ vs *T*, Figure SI3, Supporting Information) signal increases upon decreasing temperature, indicating the presence of low-lying excited states with smaller "*S*" values than the ground state, in good agreement with the dominant ferromagnetic interactions qualitatively found for **8**.

Furthermore, both complexes display frequency-dependent out-of-phase (χ_M'') signals below ~3 K, but no peaks are seen (Figure 9), indicating the possibility of single molecule magnetism behavior, albeit with a small barrier to magnetization reversal.
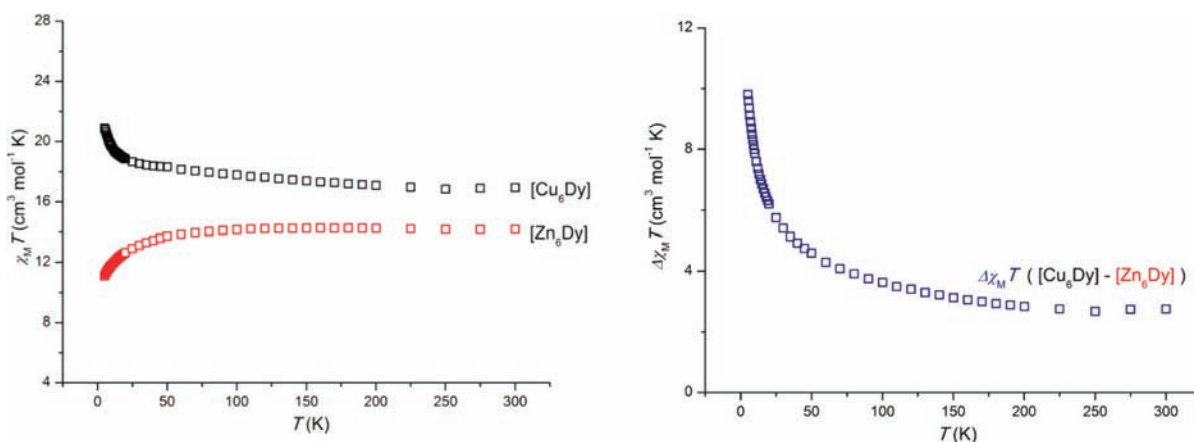

Figure 8. Plot of $\chi_M T$ vs *T* for complexes **8** and **13** under an applied dc field of 1000 G (left); plot of $\Delta\chi_M T$ vs *T* for complexes **8** and **13** (right).
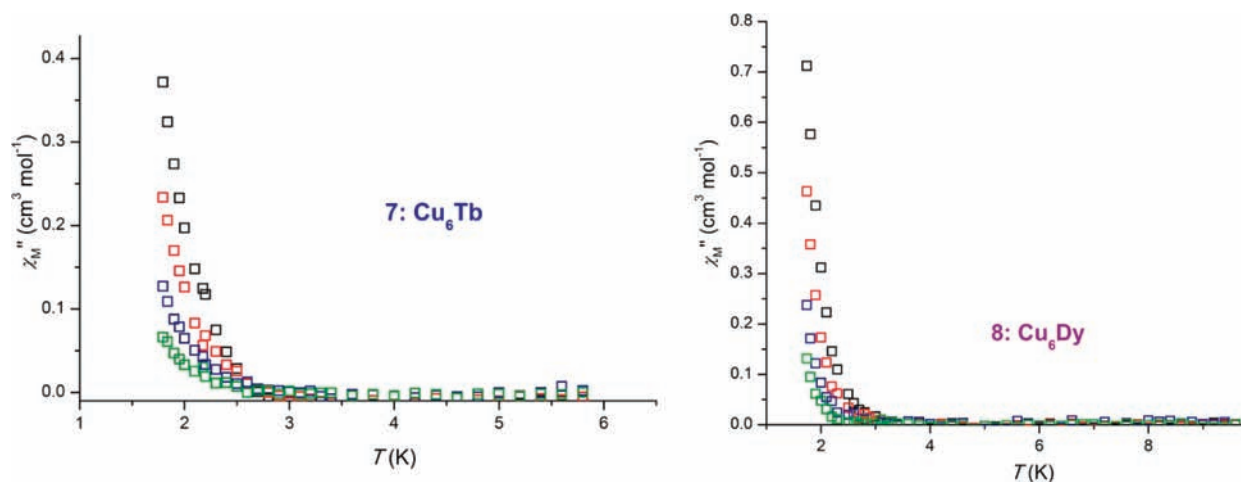
Figure 9. Plot of the out-of-phase (χ_M'') signal vs temperature for **7** (left) and **8** (right) in a 1.0 G field oscillating at 100 (green squares), 200 (blue squares), 500 (red squares), and 1000 (black squares) Hz frequency.

Thermal Decomposition Properties. Thermogravimetric analyses (TG/DTG) were carried out on a polycrystalline sample of $5\cdot6.75CH_3OH\cdot1.5Et_2O$. The thermal decomposition of complex $5\cdot6.75CH_3OH\cdot1.5Et_2O$ (Figure SI4, Supporting Information) starts with a weight loss of ~16% in the 40−114 °C region, corresponding to the loss of 6.75 mol of CH_3OH and 1.5 mol of Et_2O per mole of complex $5\cdot6.75CH_3OH\cdot1.5Et_2O$. In the 114−176 °C temperature range the plateau indicates a thermal stable product that decomposes rapidly in the 176−251 °C with a ~38% weight loss, while at higher temperature the thermal decomposition continues albeit at lower rates.

CONCLUSIONS

We have reported the syntheses, structures, and magnetic properties of 12 new heterometallic heptanuclear [Cu₆Ln] complexes based on the use of 2-amino-isobutyric acid. Among all clusters studied, complexes [Cu₆Gd] (**6**) and [Cu₆Dy] (**7**) were found to display dominant ferromagnetic interactions, with **6** having a high-spin $S = 13/2$ ground state. Furthermore, for the magnetic analysis of complex **7**, we synthesized and magnetically characterized its "Zn" analogue, [Zn₆Dy] (**13**). Finally, complexes [Cu₆Dy] (**7**) and [Cu₆Tb] (**8**) display out-of-phase ac signals, suggesting the possibility of SMM behavior.

ASSOCIATED CONTENT

S Supporting Information

Crystallographic data (CIF format) and crystallographic tables for all complexes, detailed synthesis of the [Zn₆Dy] (**13**) complex, and in-phase graphs for complexes **7** and **8**. This material is available free of charge via the Internet at http://pubs.acs.org.

AUTHOR INFORMATION

Corresponding Author
*E-mail: komil@chemistry.uoc.gr.

Notes
The authors declare no competing financial interest.

ACKNOWLEDGMENTS

REFERENCES

(1) Representative references and references therein: (a) Que, E. L.; Chang, C. J. *Chem. Soc. Rev.* **2010**, *39*, 51. (b) Fricker, S. P. *Chem. Soc. Rev.* **2006**, *6*, 524. (c) Murray, L. J.; Dincă, M.; Long, J. R. *Chem. Soc. Rev.* **2009**, *38*, 1294. (d) Manoli, M.; Collins, A.; Parsons, S.; Candini, A.; Evangelisti, M.; Brechin, E. K. *J. Am. Chem. Soc.* **2008**, *130*, 11129. (e) Bogani, L.; Wernsdorfer, W. *Nat. Mater.* **2008**, *7*, 179.

(2) (a) Milios, C. J.; Vinslava, A.; Wernsdorfer, W.; Moggach, S.; Parsons, S.; Perlepes, S. P.; Christou, G.; Brechin, E. K. *J. Am. Chem. Soc.* **2007**, *129*, 2754. (b) Rinehart, J. D.; Fang, M.; Evans, W. J.; Long, J. R. *Nat. Chem.* **2011**, *3*, 539.

(3) See, for example: (a) Karotsis, G.; Teat, S. J.; Wernsdorfer, W.; Piligkos, S.; Dalgarno, S. J.; Brechin, E. K. *Angew. Chem., Int. Ed.* **2009**, *48*, 8285. (b) Evangelisti, M; Brechin, E. K. *Dalton Trans.* **2010**, *39*, 4672. (c) Manoli, M.; Collins, A.; Parsons, S.; Candini, A.; Evangelisti, M.; Brechin, E. K. *J. Am. Chem. Soc.* **2008**, *130*, 1112.

(4) Representative references and references therein: (a) Kahn, O. *Molecular Magnetism*; VCH: New York, 1993. (b) Kahn, O.; Galy, J.; Journaux, Y. *J. Am. Chem. Soc.* **1982**, *104*, 2165. (c) Pei, Y.; Verdaguer, M.; Kahn, O.; Sletten, J.; Renard, J.-P. *J. Am. Chem. Soc.* **1986**, *108*, 428. (d) Bencini, A.; Benelli, C.; Caneschi, A.; Carlin, R. L.; Dei, A.; Gatteschi, D. *J. Am. Chem. Soc.* **1985**, *107*, 8128. (e) Benelli, C.; Caneschi, A.; Gatteschi, D.; Guillou, O.; Pardi, L. *Inorg. Chem.* **1990**, *29*, 1750. (f) Andruh, M.; Kahn, O.; Sainto, J.; Dromzee, Y.; Jeannin, S. *Inorg. Chem.* **1993**, *32*, 1623. (g) Chen, L.; Breeze, S. R.; Rousseau, R. J.; Wang, S.; Thompson, L. K. *Inorg. Chem.* **1995**, *34*, 454. (h) Costes, J.-P.; Dahan, F.; Dupuis, A.; Laurent, J.-P. *Chem.—Eur. J.* **1998**, *9*, 1617.

(5) (a) Sessoli, R.; Powell, A. K. *Coord. Chem. Rev.* **2009**, *253*, 2328. (b) Papatriantafyllopoulou, C.; Stamatatos, T.; Efthymiou, C. G.; Cunha-Silva, L.; Paz, F. A. A.; Perlepes, S. P.; Christou, G. *Inorg. Chem.* **2010**, *49*, 9743. (c) Efthymiou, C. G.; Stamatatos, T. C.; Papatriantafyllopoulou, C.; Tasiopoulos, A. J.; Wernsdorfer, W.; Perlepes, S. P.; Christou, G. *Inorg. Chem.* **2010**, *49*, 9739. (d) Mishra, A.; Wernsdorfer, W.; Parsons, S.; Christou, G.; Brechin, E. K. *Chem. Commun.* **2005**, 2086. (e) Mereacre, V.; Ako, A. M.; Clèrac, R.; Wernsdorfer, W.; Hewitt, I. J.; Anson, C. E.; Powell, A. K. *Chem.—Eur. J.* **2008**, *14*, 3577. (f) Abbas, G.; Lan, Y.; Mereacre, V.; Wernsdorfer, W.; Clèrac, R.; Buth, G.; Sougrati, M. T.; Grandjean, F.; Long, G. J.; Anson, C. E.; Powell, A. K. *Inorg. Chem.* **2009**, *48*, 9345. (g) Baskar, V.; Gopal, K.; Helliwell, M.; Tuna, F.; Wernsdorfer, W.; Winpenny, R. E. P. *Dalton Trans.* **2010**, *39*, 4747. (h) Chandrasekhar, V.; Pandian, B. M.; Boomishankar, R.; Steiner, A.; Vittal, J. J.; Houri, A.; Clèrac, R. *Inorg. Chem.* **2008**, *47*, 4918. (i) Rigaux, G.; Inglis, R.; Morrison, S.; Prescimone, A.; Cadiou, C.; Evangelisti, M.; Brechin, E. K. *Dalton Trans.* **2011**, *40*, 4797. (j) Zhang, J.-J.; Hu, S.-M.; Zheng, L.-M.; Wu, X.-T.; Fu, Z.-Y.; Dai, J.-C.; Du, W.-X.; Zhang, H.-H.; Sun, R.-Q.

Chem.—Eur. J. **2002**, *8*, 5742. (k) Zhang, J.-J.; Sheng, T.-L.; Xia, S.-Q.; Leibeling, G.; Meyer, F.; Hu, S.-M.; Fu, R.-B.; Xiang, S.-C.; Wu, X.-T. *Inorg. Chem.* **2004**, *43*, 5472. (l) Zhang, J.-J.; Xia, S.-Q.; Sheng, T.-L.; Hu, S.-M.; Leibeling, G.; Meyer, F.; Wu, X.-T.; Xiang, S.-C.; Fu, R.-B. *Chem. Commun.* **2004**, 1186. (m) Zhang, J.-J.; Sheng, T.-L.; Hu, S.-M.; Xia, S.-Q.; Leibeling, G.; Meyer, F.; Fu, Z.-Y.; Chen, L.; Fu, R.-B.; Wu, X.-T. *Chem.—Eur. J.* **2004**, *10*, 3963. (n) Hu, S.; Dai, J.; Wu, X.; Wu, L.; Cui, C.; Fu, Z.; Hong, M.; Liang, Y. *J. Cluster Sci.* **2002**, 33.

(6) See, for example: Bünzli, J.-C. G; Piguet, C. *Chem. Soc. Rev.* **2005**, *34*, 1048.

(7) Peristeraki, T.; Samios, M.; Siczek, M.; Lis, T.; Milios, C. J. *Inorg. Chem.* **2011**, *50*, 5175.

(8) (a) Orfanoudaki, M.; Tamiolakis, I.; Siczek, M.; Lis, T.; Armatas, G. S.; Pergantis, S. A.; Milios, C. J. *Dalton Trans.* **2011**, *40*, 4793. (b) Sopasis, G. J.; Orfanoudaki, M.; Zarmpas, P.; Philippidis, A.; Siczek, M.; Lis, T.; O'Brien, J. R.; Milios, C. J. *Inorg. Chem.* **2012**, *51*, 1170.

(9) Sheldrick, G. M. *Acta Crystallogr.* **2008**, *A64*, 112.

(10) (a) Zhang, Y.-J.; Ma, B.-Q.; Gao, S.; Li, J.-R.; Liu, Q.-D.; Wen, G.-H.; Zhang, X.-X. *J. Chem. Soc., Dalton Trans.* **2000**, 2249. (b) Liu, Q.-D.; Gao, S.; Li, J.-R.; Zhou, Q.-Z.; Yu, K.-B.; Ma, B.-Q.; Zhang, S.-W.; Zhang, X.-X.; Jin, T.-Z. *Inorg. Chem.* **2000**, *39*, 2488. (c) Liu, Q.-D.; Li, J.-R.; Gao, S.; Ma, B.-Q.; Kou, H.-Z.; Ouyang, L.; Huang, R.-L.; Zhang, X.-X.; Yu, K.-B. *Eur. J. Inorg. Chem.* **2003**, 731. (d) Du, W.-X.; Zhang, J.-J.; Hu, S.-M.; Xia, S.-Q.; Fu, R.-B.; Xiang, S.-C.; Li, Y.-M.; Wang, L.-S.; Wu, X.-T. *J. Mol. Struct.* **2004**, *701*, 25. (e) Du, W.-X.; Zhang, J.-J.; Hu, S.-M.; Xia, S.-Q.; Xiang, S.-C.; Wu, X.-T. *Chin. J. Struct. Chem.* **2005**, *24*, 226.

(11) Zhang, J.-J.; Hu, S.-M.; Xiang, S.-C.; Sheng, T.; Wu, X.-T.; Li, Y.-M. *Inorg. Chem.* **2006**, *45*, 7173.

(12) See, for example: (a) Leininger, S.; Fan, J.; Schmitz, M.; Stang, P. J. *Proc. Natl. Acad. Sci. U.S.A.* **2000**, *97*, 1381. (b) Shiga, T.; Newton, G. N.; Mathieson, J. S.; Tetsuka, T.; Nihei, M.; Cronin, L.; Oshio, H. *Dalton Trans.* **2010**, *39*, 4730. (c) Hamilton, T. D.; Papaefstathiou, G. S.; Friščić, T.; Bučar, D.-K.; MacGillivray, L. R. *J. Am. Chem. Soc.* **2008**, *130*, 14366. (d) Atkinson, I. M.; Benelli, C.; Murrie, M.; Parsons, S.; Winpenny, R. E. P. *Chem. Commun.* **1999**, 285.

(13) *Handbook on the Physics and Chemistry of Rare Earths*; Gschneidner, K. A., Jr., Bünzli, J.-C., Pecharsky, V. K., Eds.; Elsevier North-Holland: New York, 2009; Vol 39.

(14) Cotton, S. *Lanthanide and Actinide Chemistry*; John Wiley & Sons: West Sussex, U.K., 2006.

(15) Crawford, V. H.; Richardson, H. W.; Wasson, J. R.; Hodgson, D. J.; Hatfield, W. E. *Inorg. Chem.* **1976**, *15*, 2107.

(16) McGregor, K. T.; Hodgson, D. J.; Hatfield, W. E. *Inorg. Chem.* **1976**, *15*, 421.

(17) (a) Nishida, Y.; Kida, S. *J. Chem. Soc., Dalton Trans.* **1986**, 2633. (b) McKee, V.; Zvagulis, M.; Reed, C. A. *Inorg. Chem.* **1985**, *24*, 2914.

(18) (a) Miller, J. S.; Epstein, A. J. *Angew. Chem., Int. Ed. Engl.* **1994**, *33*, 385. (b) Benelli, C; Gatteschi, D. *Chem. Rev.* **2002**, *102*, 2369. (c) Kahn, O. *Acc. Chem. Res.* **2000**, *33*, 647. (d) Tougait, O.; Ibers, J. A. *Inorg. Chem.* **2000**, *39*, 1790. (e) Kou, H.-Z.; Gao, S.; Jin, X. *Inorg. Chem.* **2001**, *40*, 6295. (f) Costes, J.-P.; Dahan, F.; Dupuis, A.; Laurent, J.-P. *New J. Chem.* **1998**, 1525. (g) Margeat, O.; Lacroix, P. G.; Costes, J. P.; Donnadieu, B.; Lepetit, C. *Inorg. Chem.* **2004**, *43*, 4743. (h) Costes, J. P.; Dahan, F.; Dupuis, A. *Inorg. Chem.* **2000**, *39*, 165. (i) Costes, J. P.; Dahan, F.; Dupuis, A.; Laurent, J. P. *Inorg. Chem.* **1997**, *36*, 3429. (j) Ramade, I.; Kahn, O.; Jeannin, Y.; Robert, F. *Inorg. Chem.* **1997**, *36*, 930. (k) Costes, J.-P.; Dahan, F.; Dupuis, A.; Laurent, J.-P. *Inorg. Chem.* **1996**, *35*, 2400.

(19) (a) Murugesu, M.; Clèrac, R.; Pilawa, B.; Mandel, A.; Anson, C. E.; Powell, A. K. *Inorg. Chim. Acta* **2002**, *337*, 328. (b) Colacio, E.; Dominguez-Vera, J. M.; Kivekäs, R.; Moreno, J. M.; Romerosa, A.; Ruiz, J. *Inorg. Chim. Acta* **1993**, *212*, 115. (c) Colacio, E.; Costes, J.-P.; Kivekäs, R.; Laurent, J. P.; Ruiz, J. *Inorg. Chem.* **1990**, *29*, 4240. (d) Ruiz-Perez, C.; Sanchiz, J.; Hernandez-Molina, M.; Lloret, F.; Julve, M. *Inorg. Chem.* **2000**, *39*, 1363. (e) Towle, D. K.; Hoffmann, S. K.; Hatfield, W. E.; Singh, P.; Chaudhuri, P. *Inorg. Chem.* **1988**, *27*, 394. (f) Colacio, E.; Dominguez-Vera, J. M.; Costes, J. P.; Kivekas, R.; Laurent, J. P.; Ruiz, J.; Sundberg, M. *Inorg. Chem.* **1992**, *31*, 774.

(20) (a) Kahn, M. L.; Mathonière, C.; Kahn, O. *Inorg. Chem.* **1999**, *38*, 3692. (b) Costes, J.-P.; Dahan, F.; Dupuis, A.; Laurent, J.-P. *Chem.—Eur. J.* **1998**, *4*, 1616.

5918

dx.doi.org/10.1021/ic300538q | *Inorg. Chem.* 2012, 51, 5911–5918